Journal of Polymer Research (2021) 28: 149
https://doi.org/10.1007/s10965-021-02499-w

ORIGINAL PAPER

Synthesis and characterization of an isocyanate-terminated hyperbranched polymer and its waterborne study

Jie Zhang[1] · Hui-Ting Tian[1] · Yu-Ting Zhang[1] · Chun-Pu Hu[1] · Zhi-Ping Zhang[1]

Received: 15 December 2020 / Accepted: 17 March 2021 / Published online: 6 April 2021

Abstract

An isocyanate-terminated hyperbranched polymer (HBI) was successfully synthesized by reacting hyperbranched polyester (Boltorn™ HB-20) with isophorone diisocyanate (IPDI). Gel permeation chromatography (GPC) was used to monitor the molecular weight and its distribution changes during the synthesis. The structure and composition of IPDI were characterized by ^{1}H and ^{13}C nuclear magnetic resonance (NMR) spectroscopy. The structure of HBI was confirmed by one-dimensional ^{1}H, ^{13}C NMR, and distortionless enhancement by polarization transfer (DEPT) NMR spectroscopy as well as two-dimensional heteronuclear multiple bond coherence (2D-HMBC) and heteronuclear single quantum coherence (HSQC) NMR spectroscopy. Furthermore, HBI was reacted with methoxypolyethylene glycols (MPEG) to obtain a water-dispersible polyisocyanate with hyperbranched structure.

Keywords Isocyanate-terminated · Hyperbranched · Water-dispersible · 2D NMR

Introduction

Hyperbranched polymers have dendritic-like structures with many branching points and terminal reactive functional groups in their molecular structure. They have various advantages, such as high reactivity, low viscosity in solution and molten state, and good compatibility with other materials [1]. Thus, they have a wide range of applications in Ultra Violet (UV) curing materials [2–5], organic-inorganic hybrid materials [6–8], biomedical materials [9–11], engineering [12] and other fields [13, 14].

In our previous studies [15, 16], it was found that the introduction of a hyperbranched polymer HB-20 (a second generation of hyperbranched polyester) into polyester and polyether aliphatic polyurethane could significantly enhance the mechanical properties when the addition amount of HB-20 was less than 10wt%. Commercially available hyperbranched polymers mostly contain hydroxyl, amino, or carboxyl-terminated groups, which limits the use of hyperbranched polymers in polyurethanes. The isocyanate-terminated hyperbranched polymer can be prepared by modification of the hydroxyl group, and it can be very conveniently applied to preparation of polyurethane elastomers, coatings, spandex spinning and other fields by utilizing its low viscosity and good compatibility characteristics.

Waterborne technology has received more and more attention because of its environmental and pollution-free advantages. Bao [17] terminated the hyperbranched polyester HB-20 with maleic anhydride, and water-dispersible hyperbranched coatings with different properties were obtained by adjusting the proportion of triethylamine and glycidyl tertiary carbonate. Zhang [18] used maleic anhydride to block HB-40 directly, and obtained a water-dispersible hyperbranched polymer. Hu [19], Yin [20] and Lin [21] prepared UV-curable waterborne hyperbranched polyester-polyurethanes by adding triethylamine to form polymer salts. Currently, the study of waterborne hyperbranched polymers is still limited, and only simple terminated functional groups have been used.

The two-component waterborne technology [22] has received great attention, as it can improve the inherent defects of waterborne resins by post-crosslinking. Water-dispersible isocyanate is an important cross-linker. As the cations promote the reaction between water and isocyanate, the stability and storage life of products can be affected. Most of the current literature on waterborne technology is focused on the

✉ Jie Zhang
zhangjie1@ecust.edu.cn

[1] School of Materials Science and Engineering, East China University of Science and Technology, Shanghai 200237, China

grafting modification of isocyanates with methoxypolyethylene glycols, as the introduction of a hydrophilic polyglycol ether into the isocyanate structures improves the water dispersibility. Due to the low functionality of the isocyanates used, and the further decrease in their functionality after graft modification, the crosslinking effect cannot be obtained in two-component aqueous systems. Therefore, the focus is to increase the functionality of water-dispersible isocyanates.

Based on the above background, this study investigated the preparation of an isocyanate-terminated hyperbranched polymer by using the different activities of two NCO groups in IPDI, in the presence of organometallic catalyst (stannous octoate, zirconium acetylacetonate). GPC was used to monitor the molecular weight and its distribution changes during the synthesis, and the product was characterized by one-dimensional and two-dimensional NMR spectroscopy. Then, water-dispersibility polyisocyanates with hyperbranched structure were prepared by reacting isocyanate-terminated hyperbranched polyesters with methoxypolyethylene glycols.

Experimental

Materials

The hyperbranched aliphatic polyester (Boltorn^{TM} HB-20, dendritic polymerwith 16 primary hydroxyl groups theoretically and a molecular weight of 1747g.mol^{-1}) was provided by Perstorp Specialty Chemicals AB (Sweden). Isophorone diisocyanate (IPDI) was purchased from Toyo Kasei Kogyo Corporation (Japan). Methoxypolyethylene glycols (Mn = 420,540, and 660 g.mol^{-1}) were provided by LiMing Chemical Research and Design Institute Corporation (China),and were vacuum dried at 100°C for 1 h before use. Stannous octoate (Sn-cat) and zirconium acetylacetonate (Zr-cat) were provided by Aldrich Corporation(China). N,N-Dimethylacetamide (DMAc) was supplied by Shanghai Feida Industry Corporation (China), and was dried with 0.4 nm molecular sieves for one week before use. All the other reagents were used without further purification.

Synthesis of isocyanate-terminated hyperbranched polyester

Synthesis: HB-20 and DMAc (HB-20/DMAc = 1/1, w/w) were added to a 250 mL four-necked round bottom flask equipped with a mechanical stirrer, thermometer, nitrogen tubing and vacuum interface. The mixture was stirred and heated until HB-20 was completely dissolved and the resulting solution was clear and transparent. After cooling down to room temperature, stoichiometric amount of IPDI (NCO/OH=2:1 to 4:1, molar ratio) and the catalyst (0.1 wt% of the total mass) were added to the above solution. The mixture was stirred and allowed to react at room temperature. The change in NCO content was measured by N-butylamine titration until it was close to the theoretical value, and then the reaction was stopped.

Purification: Cyclohexane was added into the above reaction mixture. After thorough mixing, the homogeneous mixture was transferred into a separatory funnel and allowed to stand for separation. Excess IPDI monomer was extracted with cyclohexane repeatedly. The residual cyclohexane was then removed in vacuo to give an isocyanate-terminated hyperbranched polymer (labelled as HBI), as a white, powdered solid at room temperature. The synthesis route is shown in Scheme 1.

Synthesis of waterborne isocyanate-terminated hyperbranched polymers

First, MPEG was added to a 250 mL four-necked round-bottomed flask equipped with a mechanical stirrer, thermometer, nitrogen tubing, and vacuum interface, and then it was vacuum dried at 100°C for 1 h. After cooling down to 60°C, the as-synthesized isocyanate-terminated hyperbranched polymer (HBI) was added stoichiometrically. The mixture was slowly heated up to 90°C and reacted for 3 h. The change in NCO content was measured by N-butylamine titration until it was close to the theoretical value, and then the reaction was stopped. A light yellow, low viscosity transparent waterborne isocyanate-terminated hyperbranched polymer was obtained.

Characterization

Infrared spectroscopy was performed on a Nicolet 5700 spectrophotometer (Thermo Scientific, USA) between 4000 and 400 cm^{-1} with a resolution of 4 cm^{-1} at 25℃. The HBI sample was dissolved in acetone and cast onto a clean KBr pellet. The solvent was removed at 90℃ until no characteristic absorption peak of acetone was detected in the infrared spectrum. Finally, the FT-IR spectrum was scanned and recorded.

1D and 2D NMR spectra were recorded on a 500 MHz superconducting Fourier transform NMR spectrometer (Bruker Instrument Corporation, Germany) in dimethyl sulfoxide d6 (DMSO-d6) or chloroform-d with Me_4Si (TMS) as the internal standard at room temperature.

Gel Permeation Chromatography was performed on a Waters 1515 Isocratic HPLC instrument (Waters Corporation, USA) in tetrahydrofuran with a flow rate of 1 mL/min and sample concentration of 4.5 mg/ml at 35℃.

Scheme 1 Schematic description of the synthesis for HBI

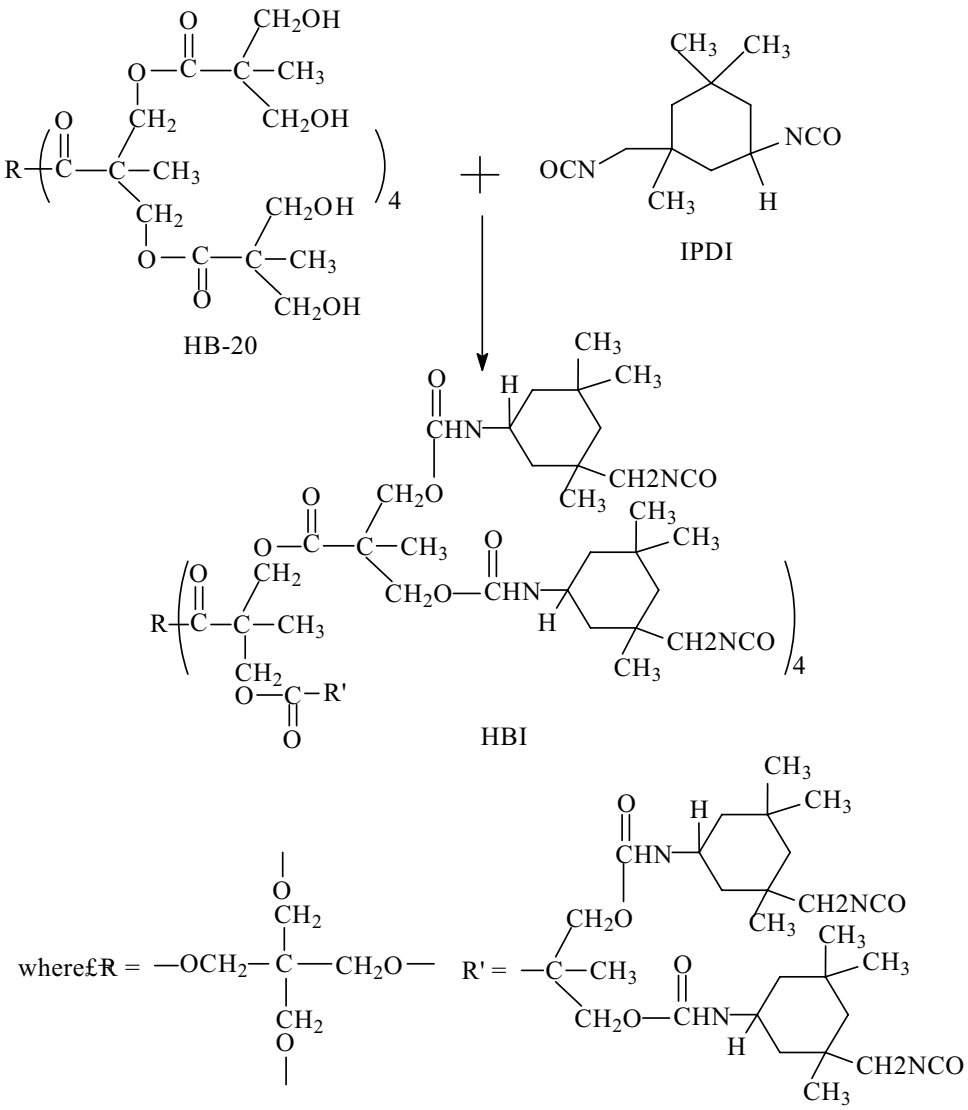

Results and discussion

Synthesis of isophorone diisocyanate terminated hyperbranched polymer (HBI)

HBI was synthesized with HB-20 (f=16) and IPDI (f=2) as the starting materials in a simple process, in which chain extension and cross-linking reactions were the main side reactions. The type of catalyst and the reaction temperature had a significant influence on the reactivity of primary and secondary NCOs in IPDI [23, 24, 25].In the presence of organometallic catalysts and low temperature, the difference in the activity of the two NCOs increased. In order to reduce the side reactions and obtain products with uniform molecular weight distribution, we selected stannous octoate and zirconium acetylacetonate as catalysts and performed the synthesis at a lower temperature. Also, the ratio of the reactants was investigated.

Table 1 The conditions and phenomenon for the synthesis for HBI[a]

Sample	NCO/OH (molar ratio)	HB-20/IPDI (wt/wt)	HBI contents (wt%)	Average functionality for NCO	Phenomenon
1	2:1	100/189.3	100.0	16.0	gel in the synthesis
2	3:1	100/284.0	75.3	2.8	gel after the synthesis
3	4:1	100/378.6	60.5	2.6	buff clear liquid

[a]Catalyst: stannous octoate; reaction temperature: 30℃

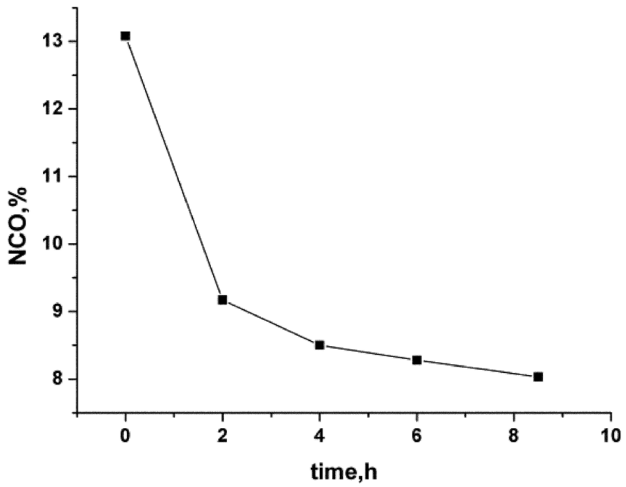

Fig. 1 NCO vs time for reaction of HB-20 and IPDI (NCO/OH = 4:1, molar ratio)

Firstly, the effect of molar ratio on the reaction was examined in the presence of stannous octoate catalyst and reaction temperature of 30℃. The results are shown in Table 1. The change in NCO content with time was monitored by di-n-butylamine titration, as shown in Fig. 1. As can be seen from Table 1, when the molar ratio of NCO and OH was less than 3, the cross-linking reaction could easily occur, resulting in a gel product. As seen from Fig. 1, the reaction time should be at least 8 h to ensure sufficient conversion.

Based on the above results, the molar ratio of NCO and OH was fixed at 4:1, and the effects of the two catalysts (stannous octoate and zirconium acetylacetonate) on the reaction were studied. GPC was used to characterize the products' molecular weight and molecular weight distribution. The experimental results are shown in Table 2. When zirconium acetylacetonate was used as the catalyst, the HBI product had the narrowest molecular weight distribution at 30°C reaction temperature, and the experiments had good repeatability (the results of samples 3# and 4# were very close in Table 2). Also, it can be seen that at higher synthesis temperatures, the resulting product had a higher molecular weight and a broader weight distribution, even when the molar ratio of NCO/OH was further increased to 4.6:1. This is likely due to an increasement in side reactions. When the reaction temperature was high, the reactivities of the two NCOs in IPDI were similar and the selectivity of the two NCOs decreased. Consequently, the cross-linking reaction between the hyperbranched structures increased, resulting in an increase in the average molecular weight and a broadening of the distribution.

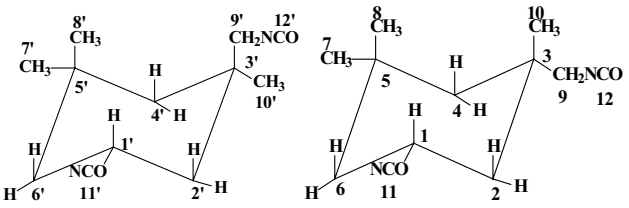

Scheme 2 Structure of cis-IPDI and trans-IPDI

In summary, the optimal synthesis conditions were determined to be: Zr-cat as the catalyst, 4:1 molar ratio of NCO/OH, and reaction temperature of 30°C. Under these conditions, storage-stable HBI could be synthesized. The structures of IPDI and HBI were further characterized by 1D and 2D NMR.

Structural characterization of IPDI

IPDI is a six-membered alicyclic diisocyanate in which the ratio of cis- and trans- stereoisomers is 75:25 [23]. Also, the two isocyanate groups in the structure were primary and secondary NCO groups with a large difference in reactivity. Scheme 2 shows the stereoisomerism of IPDI. ^{1}H NMR and ^{13}C NMR were performed to determine the structural composition of IPDI. The characteristic absorption peaks of IPDI in the ^{1}H spectrum (Fig. 2) and the ^{13}C spectrum (Fig. 3) were assigned in a previous work[26] and the results are shown in Table 3.

In the ^{1}H NMR spectrum, the peaks from 3.0 to 3.4 ppm were assigned to two H protons in -CH_2NCO (primary NCO). According to the integral area of the peak intensity, the ratio of the cis and trans isomers could be calculated as 77.8:22.2. The peaks from 3.4 to 3.75 ppm were assigned to the H proton in –CHNCO (secondary NCO) and the ratio of cis and trans isomers was 77.5:22.5. As can be seen, both calculations were close. The ratio of cis and trans isomers was further confirmed by ^{13}C NMR spectroscopy. In the ^{13}C NMR spectrum, the peak at 23.64 ppm was assigned to

Table 2 Synthesis results for HBI

Sample	Catalysts	Reaction temp.℃	NCO/OH, molar ratio	Mn	Mw	Mw/Mn
HB-20	/	/	/	3277	4238	1.29
1#	Sn	70	4.6:1	173728	236297	2.38
2#	Sn	30	4:1	8839	18758	2.12
3#	Zr	30	4:1	8875	14539	1.64
4#	Zr	30	4:1	8609	14411	1.67

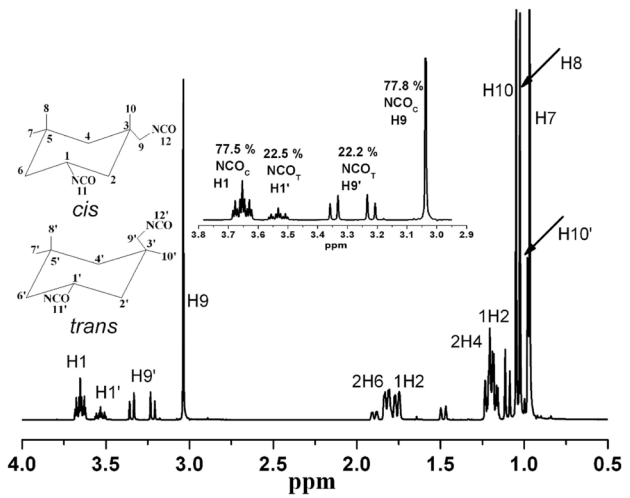

Fig. 2 ^{1}H NMR spectrum of IPDI [1]

C (10) with an intensity of 0.97, and the peak at 30.19 ppm was assigned to C (10') with an intensity of 0.28. The content of the cis-structure was calculated as 77.6 wt%, while the content of the trans-structure was 22.4 wt%, which is in good agreement with the ^{1}H NMR spectrum.

Structural characterization of HBI

One-dimensional NMR spectrum analysis

Both primary NCO and secondary NCO in IPDI can react with hydroxyl groups in HB-20 to form carbamate groups (-NH-COO-). The structure of HBI can be seen in Scheme 3.

In the ^{1}H NMR and ^{13}C NMR spectra, the formation of carbamate group influenced the signals of hydrogen protons linked to C1, C2, C3, C4, C6, and C9 in the IPDI fatty ring, and the -CH_2-signals linked to the hydroxyl groups in HB-20. Also, the ^{13}C signals of the two NCOs (C11 and C12) were affected and a peak corresponding to the carbon atom in urethane carbonyl groups appeared. The ^{1}H and ^{13}C peaks of other units in the molecule were less affected.

Figures 4 and 5 show the ^{1}H NMR and ^{13}C NMR spectra of HBI, respectively. According to the structural analysis of IPDI and HB-20 [27], the attribution of chemical shift peaks was initially indicated in Figs. 4 and 5. It can be seen that the spectra contain signal peaks of related atoms in the structures of IPDI and HB-20 [27]. In the ^{13}C NMR spectrum, the peak at 155.29 ppm was assigned to the carbon atom in the carbamate formed by the reaction of NCO group in IPDI with HB-20, which shifted from 120 ppm to 155.29 ppm because of the deshielding effect.

Due to the complex molecular structure of HBI, one-dimensional NMR spectra alone could not clearly characterize the structure of HBI. Thus, it was necessary to further characterize HBI with DEPT135 and 2D NMR techniques. The distortionless enhancement by polarization transfer technique (DEPT135) can distinguish the order of carbon atoms in the ^{13}C NMR spectrum. Therefore, the types of carbon atoms in HBI were first characterized by DEPT135, and then the ^{13}C NMR and DEPT135 spectra were compared in Fig 6.

As can be seen from Fig. 6, the peak at 17.91 ppm was assigned to the CH_3 carbon (a) in the HB-20 structure; the peaks at 23.39, 30.16, 27.59 and 29.31 ppm were assigned to the four CH_3 carbons (C10, C10', C8, and C8'); the peak at 34.98 ppm was assigned to the CH_3 carbon(C7); and the

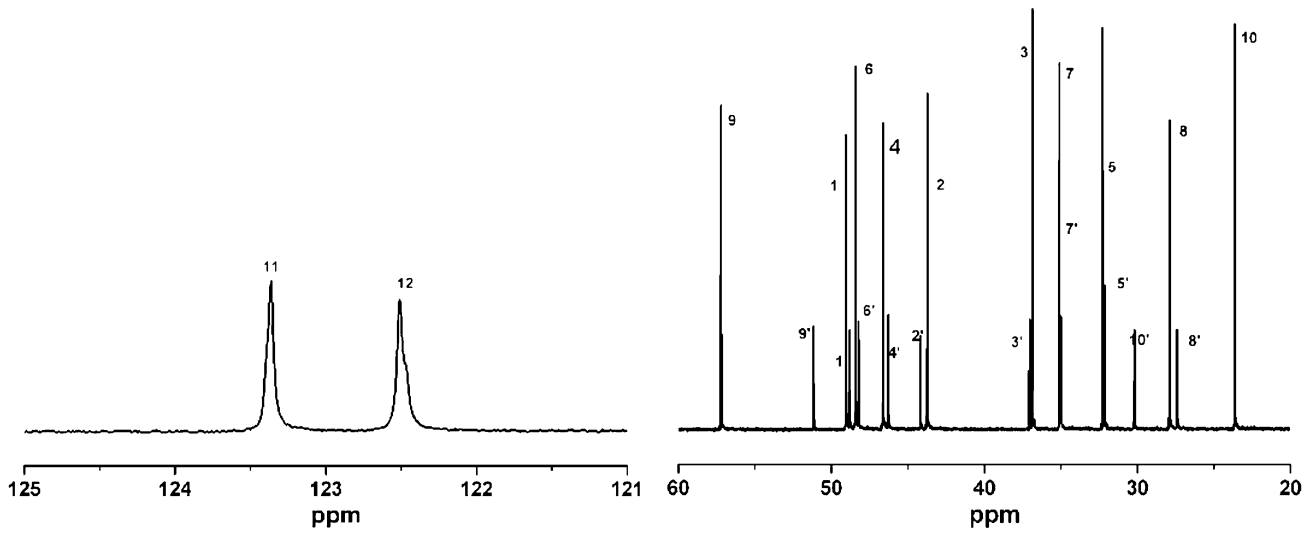

Fig. 3 ^{13}C NMR spectrum of IPDI [1]

Table 3 Assignment of IPDI peaks in ^{1}H and ^{13}C NMR spectra [1]

No.	Cis-		No.	Trans-	
	δ_H	δ_C		δ_H	δ_C
1	3.65	49.05	1’	3.53	48.80
2	1.00~1.23, 1.63~1.86	44.17	2’	1.00~1.23, 1.63~1.86	43.73
3		36.87	3’		37.04
4	1.00~1.23	46.63	4’	1.00~1.23	46.28
5		32.26	5’		32.12
6	1.63~1.86	48.43	6’	1.63~1.86	48.22
7	0.97	35.09	7’	0.97	34.98
8	1.03	27.90	8’	1.03	27.40
9	3.04	57.20	9’	3.21~3.36	51.15
10	1.05	23.64	10’	0.98	30.19
11		123.36	11’		123.36
12		122.50	12’		122.50

peak at 48.55 ppm was assigned to the CH carbon(C1). All these peaks appeared positive in the DEPT135 spectrum. Two peaks at 31.85 and 36.56 ppm disappeared in the DEPT135 spectrum, which were assigned to the quaternary carbons of C5 and C3. The peaks at 41.36, 45.93, 46.64, 53.91and 57.04 ppm were assigned to the CH_2 carbons (C2, C4, C6, C9’and C9), and the peaks from 61.92 to 67.05 ppm and 68.20 to 72.15 ppm were assigned to CH_2 carbon from HB-20; these peaks were negative in the DEPT135 spectrum. According to the above analysis, the peaks in the ^{13}C NMR spectrum of HBI were classified by DEPT135 spectrum, which was helpful for the further analysis of 2D NMR spectra.

2D-NMR HSQC spectrum and HMBC spectrum analysis

Although the H protons and carbon atoms in HBI were already assigned by one-dimensional NMR, the ^{13}C-^{1}H coupling information and the C-C bond relationship of directly connected and separated 2 to 3 chemical bonds could not be identified by ^{1}H, ^{13}C and DEPT135 spectra. It was necessary to use 2D-NMR analysis (HSQC and HMBC) to determine the molecular skeleton structure of HBI.

Fig 7 presents the high-field HSQC spectrum of HBI. The peak at 17.91 ppm in the ^{13}C spectrum was related to the peak at 1.26 ppm in the ^{1}H spectrum, which was attributed to $-CH_3$ group in HB-20. The peaks at 23.39 ppm, 27.59 ppm and 34.98 ppm in the ^{13}C spectrum were related to the peaks at 1.10 ppm, 1.08 ppm and 0.96 ppm in the ^{1}H spectrum, respectively, and were attributed to C10, C8, and C7 in IPDI. According to the above analysis, the $-CH_3$ groups of HBI from HB-20 and IPDI in the ^{13}C and ^{1}H NMR spectra were clearly characterized, which provided a basis for further quantitative calculation of the structural parameters of HBI.

Figure 8 shows the low-field HSQC spectrum of HBI. The peaks at 53.91 ppm and 57.04 ppm in the ^{13}C spectrum were related to the peaks at 2.64 ppm and 3.03 ppm in the ^{1}H spectrum, respectively, which were attributed to C9 and C9’ in IPDI. The group of peaks at 65.56 ppm in the ^{13}C spectrum was related to the group of peaks at 4.12 ppm in the ^{1}H spectrum, corresponding to $-CH_2O-$ units in HB-20. The group of peaks at 69.17 ppm in the ^{13}C spectrum was related to the group of peaks at 3.60 ppm in the ^{1}H spectrum, which was attributed to the $-CH_2-$ bonds linked to urethane in HB-20. Thus, the CH_2 groups of HBI in ^{13}C and ^{1}H NMR spectra were clearly

Scheme 3 Structure of HBI

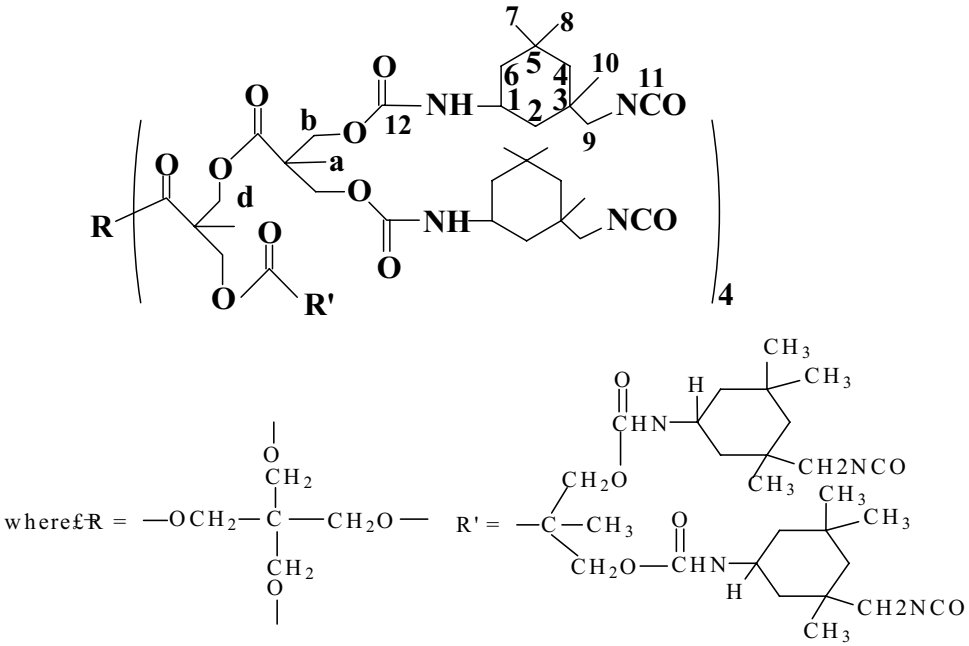

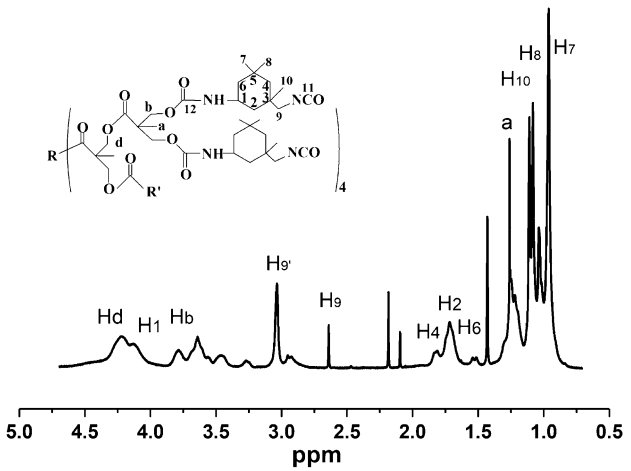

Fig. 4 ^{1}H NMR spectrum of HBI

characterized and assigned. Compared to ^{1}H NMR spectra of HB-20 [14], the peaks of Hb and Hd in Fig 4 became broader and shorter. This was due to the weakening of the H proton signal of CH_2 group after the reaction of HB-20 with IPDI.

Figures 9 and 10 present the HMBC spectra of HBI. It can be seen from Fig 9 that the peak at 121.87 ppm in the ^{13}C spectrum was related to the peak at 3.03 ppm in the ^{1}H spectrum, which was a long-range correlation between primary NCO (C11) and C9 (CH_2). Also, there was no C12 (secondary NCO) signal in Fig. 9, indicating that under the experimental conditions, the more reactive secondary NCO reacted with OH group and disappeared.

In Fig. 10, the peak at 0.96 ppm (H7) in the ^{1}H spectrum intersected with the peaks at 27.58 ppm and 31.85 ppm in the ^{13}C spectrum, corresponding to the long-range correlations between C7 and C5, C8, respectively. The peak at 1.08 ppm (H8) in the ^{1}H spectrum matched with the peaks at 31.85 ppm and 34.98 ppm in the ^{13}C spectrum, which were the long-range correlations between C8 and C5, C7, respectively. The peak at 1.10 ppm (H10) in the ^{1}H spectrum intersected with the peaks at 36.56, 41.36, 45.93, and 57.04 ppm in the ^{13}C spectrum, which were the long-range correlations between C10 and C3, C2, C4 and C9, respectively. The above correlations indicated the positional relationships of the groups in IPDI, and the correlation peaks in the ^{13}C and ^{1}H NMR spectra were assigned.

In addition, it was also noted from Fig. 10 that the peak at 1.26 ppm (-CH_3 in HB-20) in the ^{1}H spectrum matched with the peaks at 29.31, 53.91, and 69.54 ppm in the ^{13}C spectrum, respectively, corresponding to the long-range correlations between -CH_3 and C8', C9, and -CH_3(position d). Further analysis was required to confirm whether the long-range correlations between these distant groups were related to the hyperbranched spatial structure.

According to the above analysis, the peaks in the ^{13}C spectrum of HBI introduced by IPDI remained unchanged, except for the dwarfing of peaks C1, C2, C4, and C6. This result indicated that the reaction between HB-20 and IPDI had occurred to form an IPDI-terminated isocyanate hyperbranched polymer, and that the hyperbranched polyester was surrounded by IPDI. In addition, the peak of the secondary NCO (C12) almost disappeared compared to the peak of the primary NCO (C11), and the carbonyl peak appeared at 155.29 ppm. At the same time, the peak of H9 (H9') still showed a high intensity in the ^{1}H spectrum, indicating that the secondary NCO in IPDI had higher reactivity under the synthesis conditions. The complete assignment of chemical shift peaks for HBI in ^{1}H and ^{13}C spectra are summarized in Table 4.

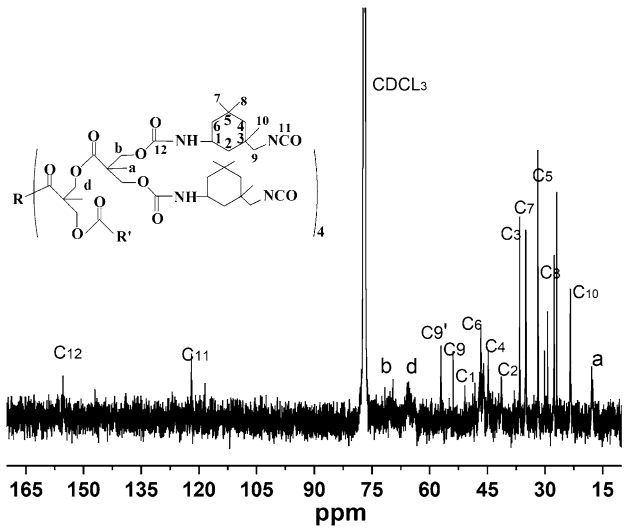

Fig. 5 ^{13}C NMR spectrum of HBI

Molecular weight distribution of HBI

The molecular weight distributions of HBI and HB-20 were characterized by GPC and the results are shown in Fig. 11. It can be seen that the GPC chromatogram of HBI showed a unimodal distribution, and the molecular weight distribution was slightly wider than that of HB-20, indicating that the crosslinked structure was low in HBI.

Molecular weight of HBI

Due to the smaller hydrodynamic volume of the hyperbranched structure, the determination of the molecular weight by GPC with polystyrene as the standard sample had a large deviation. Therefore, according to the above structural analysis of HBI, combined with the ^{1}H NMR data, the molecular weight of HBI was quantitatively calculated.

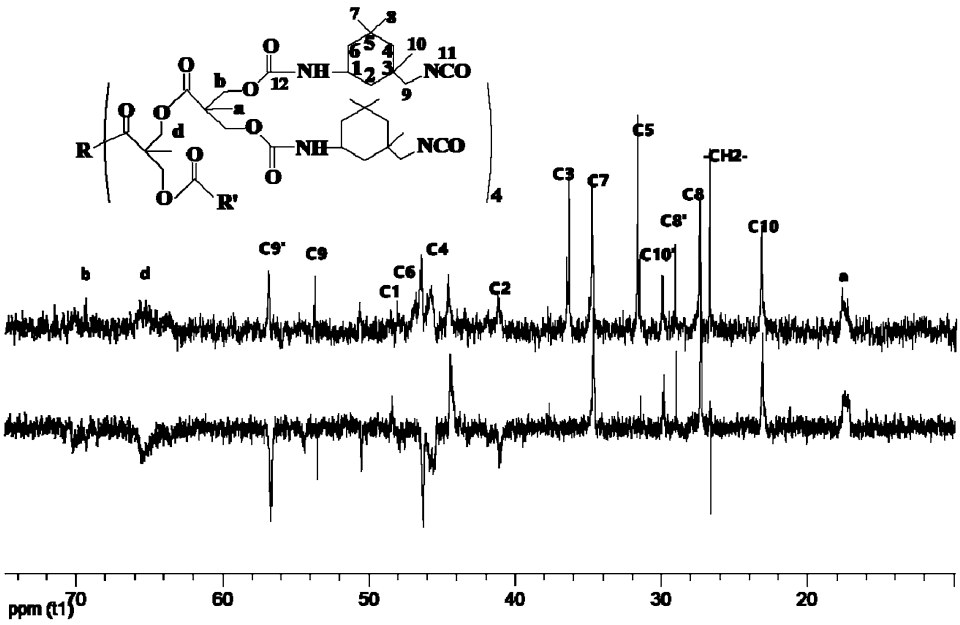

Fig. 6 ^{13}C NMR (upper) and DEPT135 (down) spectra of HBI

In the ^{1}H spectrum of HBI, the relative integral area ratio of $-CH_3$ groups in hyperbranched structure (the peaks from 1.16 to 1.34 ppm) and $-CH_3$ groups in IPDI (the peaks from 0.85 to 1.16 ppm) was 1:3.05. There were 3 $-CH_3$ groups in IPDI, and it can be concluded that each structural unit (Dimethylol Propionic Acid (DMPA)) includes one IPDI structure.

There are 15 DMPA structures in each HB-20 from the above calculations 27. Thus, the hydroxyl terminated hyperbranched polyester had completely reacted with IPDI, forming an NCO-terminated hyperbranched polymer with functionality of 15, and its molecular weight is: $15 \times 222.27 + 1876 = 5210$ g/mol.

The NCO content in HBI could be further calculated as 12.1% (15×42×100/5210). Also, the experimentally measured NCO content in HBI was 10.8%, which is close to the calculated value. These results confirmed that the NCO-terminated hyperbranched isocyanate was synthesized and the waterborne study of HBI could be further performed.

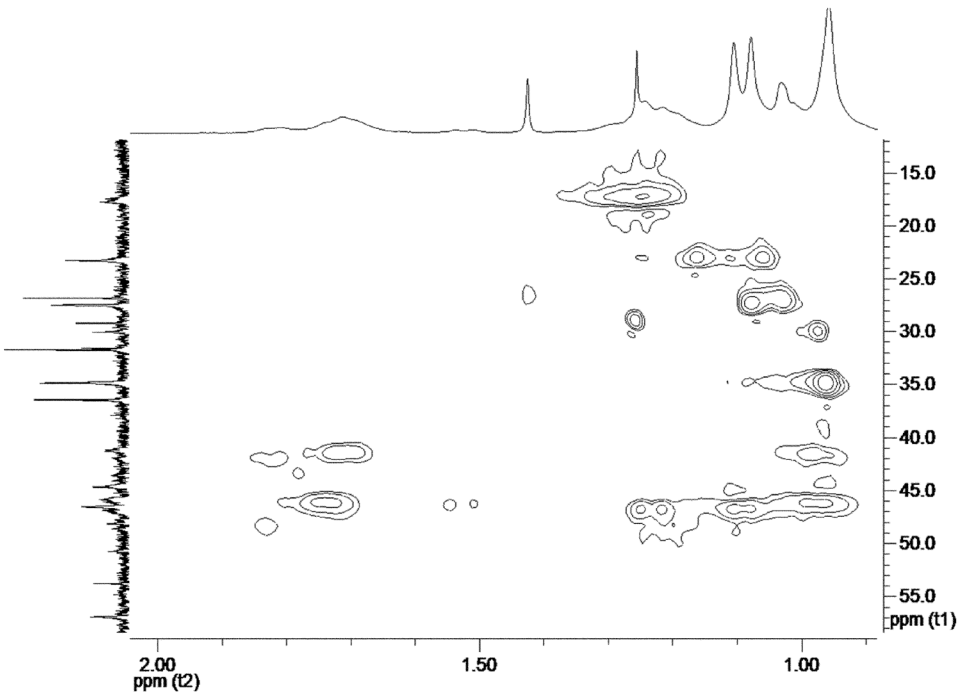

Fig. 7 HSQC spectrum of HBI in high field

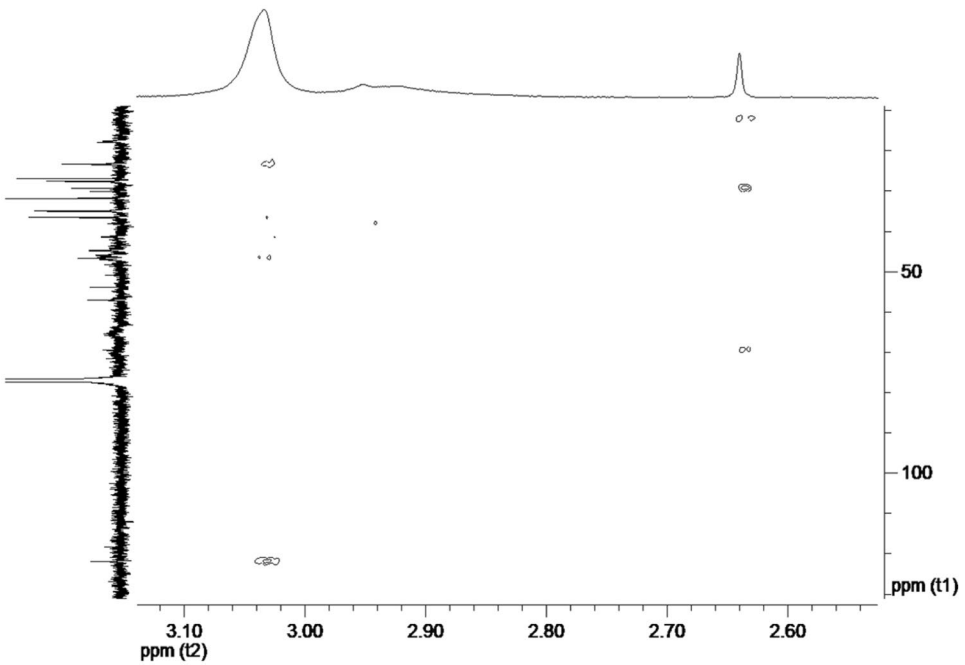

Fig. 8 HSQC spectrum of HBI in low field

Waterborne study of HBI

Xing and Ye [28] performed the waterborne study of aromatic isocyanates (Polymeric Methylenediphenyl Diisocyanate) and aliphatic isocyanates (Hexamethylene Diisocyanate trimers and IPDI trimers), and found that the use of mono-terminated polyethylene glycol ether as the aqueous reagent was a better choice, as the capping agent played an important role in the stability of the waterborne polyisocyanate. Moreover, the length of the hydrophilic polyethylene glycol segments also affects the product and a moderate chain length is recommended. The waterborne polyisocyanate was solid at room temperature if the chain was too long, which limited its use; and the stability of the waterborne polyisocyanate declined if the chain was too short. In this study, three different single-terminated polyglycol ethers with molecular weights of 420, 540, and 660 were selected as the hydrophilic agents, and HBI was used to synthesize waterborne HBI (WHBI). The stability

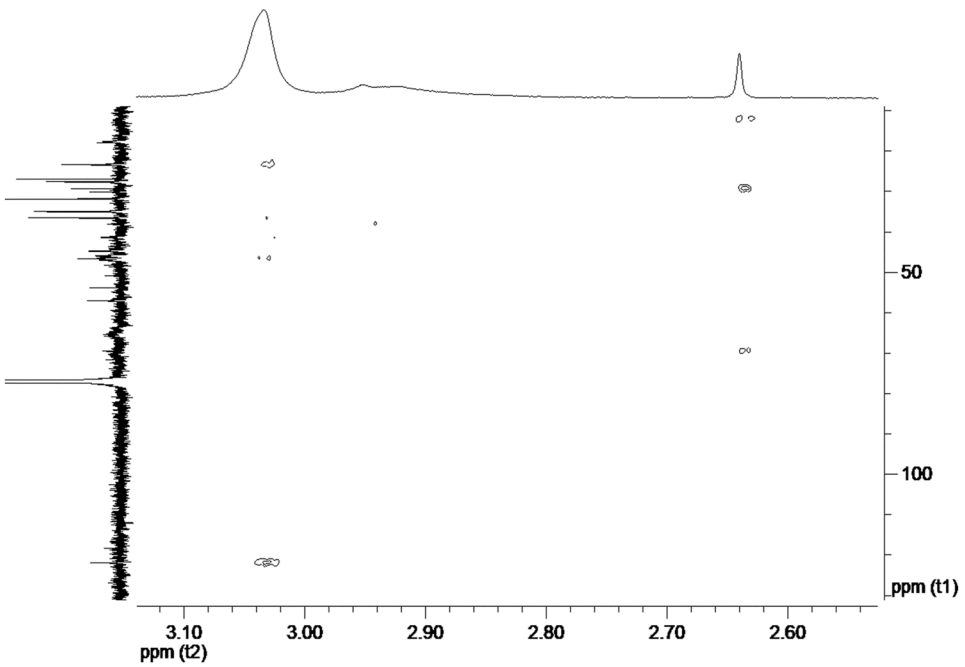

Fig. 9 HMBC spectrum of HBI in sub-high field

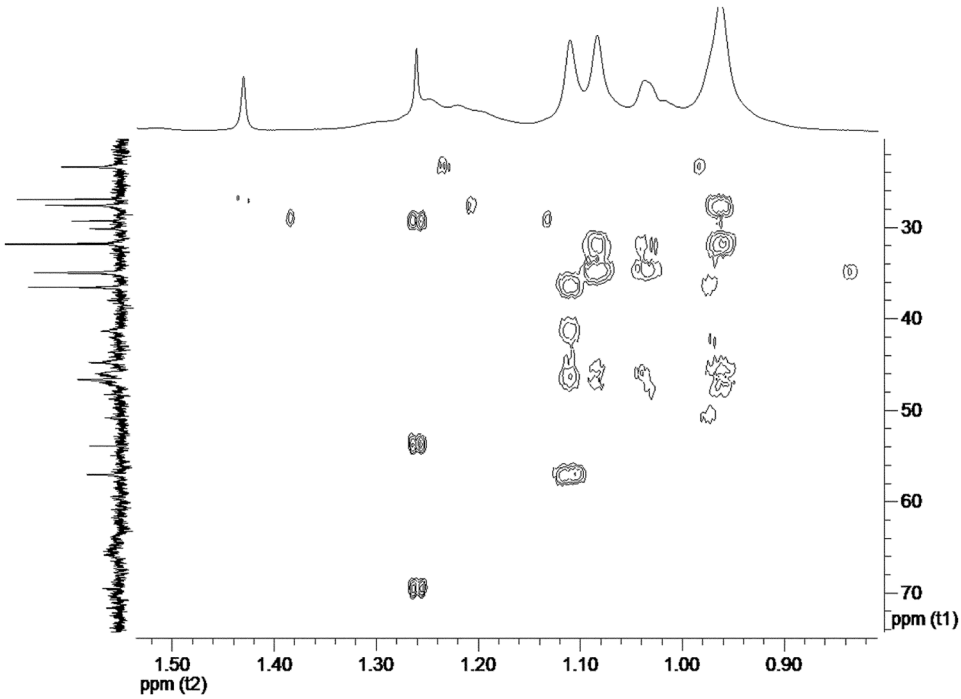

Fig. 10 HMBC spectrum of HBI in high field

and dispersibility of the hyperbranched isocyanate polymers in water were examined. The synthetic route is shown in Scheme 4, and the experimental results are shown in Table 5.

As shown in Table 5, when the amount of MPEG was small (MPEG-420, 22.3 wt%), the dispersion had poor mechanical stability and was severely separated after centrifugation due to the low content of hydrophilic groups. When the amount of MPEG-420 was increased to 36.5 wt%, a dispersible waterborne dispersion was obtained. However, the dispersion easily turned to gel, possibly because the hydrophilic layer surrounding the waterborne particles was thin and the NCO groups could not be completely enclosed in the particles. Thus, the NCO groups easily reacted with water to form gel and generate CO_2. When the molecular weight of MPEG was increased to 660 and the amount was more than 30 wt%, a stable waterborne dispersion was obtained and the storage stability of WHBI at room temperature was

Table 4 ^{1}H and ^{13}C chemical shifts of HBI

δ_C	Assignment	δ_H	Assignment
17.91	-CH3(a)	1.25	-CH3(a)
26.93	-CH2-	1.42	-CH2-
48.55	C1	0.96	H7
41.36	C2	1.08	H8
36.56	C3	2.64	H9
45.93	C4	3.03	H9’
31.85	C5	1.10	H10
46.64	C6	1.03	H10’
34.98	C7		
27.59	C8		
29.31	C8’		
53.90	C9		
57.04	C9’		
23.39	C10		
30.17	C10’		
121.87	C11		
155.29	C12		
172.76	-C=O		
61.92~67.05	-CH2(b)		
68.20~72.15	-CH2(d)		

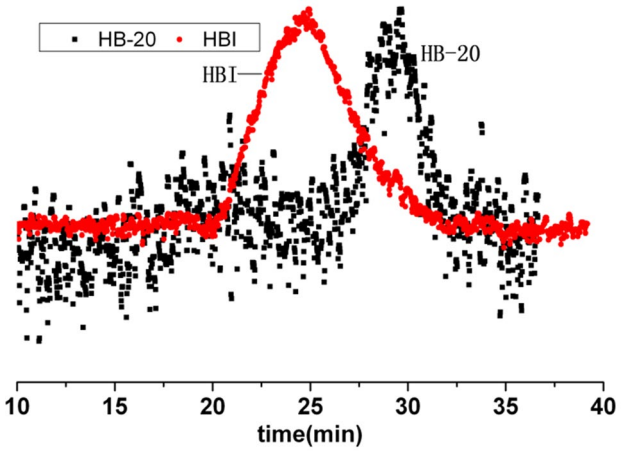

Fig. 11 GPC spectra of HBI and HB-20

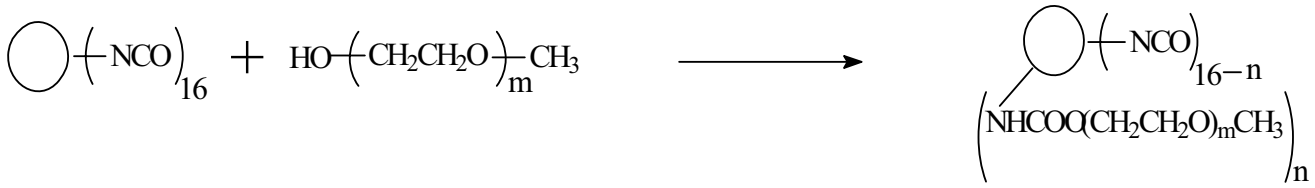

Scheme 4 Synthetic process of WHBI

Table 5 Results of WHBI dispersed in water

Sample	MPEG-420 (wt %)	MPEG-540 (wt %)	MPEG-660 (wt %)	Average function ality	Appearance and stability of water dispersion of WHBI		
					Appearance	After storing 30 min	Stability[a]
WHBI-1	22.3			11.5	white dispersion	minor bubbles	significant precipitation
WHBI-2	36.5			7.9	milky clear dispersion	gel	no precipitation
WHBI-3	46.4			4.3	blue clear dispersion	lots of bubbles	no precipitation
WHBI-4		19.8		12.6	milky dispersion	stable	minor precipitation
WHBI-5		42.5		7.9	clear dispersion	lots of bubbles	no precipitation
WHBI-6		52.6		4.3	clear dispersion	lots of bubbles	no precipitation
WHBI-7			31.1	11.5	milky blue dispersion	stable	trace precipitation
WHBI-8			47.6	7.8	clear dispersion	stable	no precipitation
WHBI-9			57.6	4.3	clear dispersion	stable	no precipitation

[a]WHBI:H_2O = 1:1 (wt/wt) , high-speed dispersion: 2 min / 1500~2000 rpm and then high-speed centrifugal separation: 10 min / 2500 rpm

more than 6 months (evaluated by centrifugal separation: 10 min/2500 rpm). The application of such hyperbranched polymers remains to be further studied.

Conclusions

1. By careful selection of catalyst, reaction temperature, reaction time and molar ratio of NCO/OH, the reaction between HB-20 and IPDI could be controlled, and a structurally-defined NCO-terminated hyperbranched polymer was successfully synthesized.
2. The structures of NCO-terminated hyperbranched polymers were characterized by ^{1}H, ^{13}C, DEPT135 NMR and two-dimensional NMR spectra (HMBC, HSQC). The molecular weights and distributions were determined by GPC (polydispersity index was 1.6 to 1.7). The synthesized NCO-terminated hyperbranched polyisocyanate had a low cross-linked structure and good storage stability.
3. A waterborne study was performed on the hyperbranched polyisocyanates with non-ionic hydrophilic polyethylene glycol. When the molecular weight of hydrophilic polyethylene glycol was more than 660 and the amount was more than 30 wt%, a waterborne hyperbranched polyisocyanate was obtained, which was stable for a storage period of more than 6 months.

Funding This study was supported by Shanghai Leading Academic Discipline Project (No.B 502).

Declarations

Conflict of interest No conflict of interest exits in the submission of this manuscript, and manuscript was approved by all authors for publication. We declared that materials described in the manuscript, including all relevant raw data, will be freely available to any scientist wishing to use them for non-commercial purposes, without breaching participant, confidentiality.

References

1. Inoue K (2000) Functional dendrimers, hyperbranched and star polymers. Prog Polym Sci 25 (4):453-571. https://doi.org/10.1016/S0079-6700(00)00011-3
2. Wei D, Liao B, Huang J et al (2019) Fabrication of castor oil-based hyperbranched urethane acrylate UV-curable coatings via thiol-ene click reactions. Prog Org Coat 135:114-122. https://doi.org/10.1016/j.porgcoat.2019.05.039

3. Wei D, Huang X, Zeng J et al (2020) Facile synthesis of a castor oil-based hyperbranched acrylate oligomer and its application in UV-curable coatings. J Appl Polym Sci 137 (36). https://doi.org/10.1002/app.49054
4. Perocheau Arnaud S, Hashemi P, Mischnick P et al (2020) Optimized synthesis of highly reactive UV-curable hyperbranched polyester acrylates. J Coat Technol Res 17 (1):127-143. https://doi.org/10.1007/s11998-019-00247-w
5. Xiang H, Wang X, Xi L et al (2018) Effect of soft chain length and generation number on properties of flexible hyperbranched polyurethane acrylate and its UV-cured film. Prog Org Coat 114:216-222. https://doi.org/10.1016/j.porgcoat.2017.10.019
6. Duarah R, Karak N (2018) High performing smart hyperbranched polyurethane nanocomposites with efficient self-healing, self-cleaning and photocatalytic attributes. New J Chem 42 (3):2167-2179. https://doi.org/10.1039/c7nj03889e
7. Zhong H, Gao X, Zhang X et al (2020) Improving the shale stability with nano-silica grafted with hyperbranched polyethyleneimine in water-based drilling fluid. J Nat Gas Sci Eng 83. https://doi.org/10.1016/j.jngse.2020.103624
8. Hou LR, Gao J, Ruan H et al (2020) Mechanical and thermal properties of hyperbranched poly(epsilon-caprolactone) modified graphene/epoxy composites. J Polym Res 27 (2). https://doi.org/10.1007/s10965-020-2008-x
9. Shan P, Chen N, Hao C et al (2020) Facile and solvent-free synthesis of a novel bio-based hyperbranched polyester with excellent low-temperature flexibility and thermal stability. Industrial Crops and Products 148. https://doi.org/10.1016/j.indcrop.2020.112302
10. Duarah R, Deka A, Karak N (2020) Multifaceted bioinspired hyperbranched polyurethane nanocomposite as a non-contact triggered self-healing material. Express Polym Lett 14 (6):542-555. https://doi.org/10.3144/expresspolymlett.2020.44
11. Aly KI, Abdel-Rahman MA, Qutai MM (2018) Photoactive linear and hyperbranched polyesters based on 4-methylcyclohexanone and 4-tert-butylcyclohexanone moieties in the main chain: synthetic methodology, characterization and cytotoxicity. J Polym Res 25 (8):15. https://doi.org/10.1007/s10965-018-1579-2
12. Guo PF, Zhang ZL, Zhang YW et al (2020) Controllable synthesis of terminal carboxyl hyperbranched polyester and their retarding effect on concrete. J Polym Res 27 (8):9. https://doi.org/10.1007/s10965-020-02188-0
13. Jovicic M, Radicevic R, Pavlicevic J et al (2020) Synthesis and characterization of ricinoleic acid based hyperbranched alkyds for coating application. Prog Org Coat 148. https://doi.org/10.1016/j.porgcoat.2020.105832
14. Zhang J, Ren H, Chen P et al (2019) Preparation and properties of waterborne polyurethane with star-shaped hyperbranched structure. Polymer 180. https://doi.org/10.1016/j.polymer.2019.121690
15. Zhang J, Hu CP (2009) Synthesis, characterization and mechanical properties of polyether-based aliphatic polyurethane elastomers composed of hyperbranched polyester segments. Acta Polymerica Sinica (9):867-873. https://doi.org/10.3321/j.issn:1000-3304.2009.09.004
16. Zhang J, Hu CP (2008) Synthesis, characterization and mechanical properties of polyester-based aliphatic polyurethane elastomers containing hyperbranched polyester segments. Eur Polym J 44 (11):3708-3714. https://doi.org/10.1016/j.eurpolymj.2008.08.019
17. Bao C-L, Wang L-S, Zhang A-Q (2009) Synthesis and properties of waterborne hyperbranched aliphatic polyester clear coats. J Taiwan Inst Chem E 40 (2):174-179. https://doi.org/10.1016/j.jtice.2008.07.013
18. Zhang Q-Z, Li B-B, Sun D et al (2016) Preparation and characterization of PVA membrane modified by water-soluble hyperbranched polyester (WHBP) for the dehydration of n-butanol. J Appl Polym Sci 133 (24). https://doi.org/10.1002/app.43533
19. Hu H, Yuan Y, Shi W (2012) Preparation of waterborne hyperbranched polyurethane acrylate/LDH nanocomposite. Prog Org Coat 75 (4):474-479. https://doi.org/10.1016/j.porgcoat.2012.06.007
20. Yin W, Zeng X, Li H et al (2011) Synthesis, photopolymerization kinetics, and thermal properties of UV-curable waterborne hyperbranched polyurethane acrylate dispersions. J Coat Technol Res 8 (5):577-584. https://doi.org/10.1007/s11998-011-9338-x
21. Lin X, Zhang S, Qian J (2014) Synthesis and properties of a novel UV-curable waterborne hyperbranched polyurethane. J Coat Technol Res 11 (3):319-328. https://doi.org/10.1007/s11998-013-9520-4
22. Fiori DE (1997) Two-component water reducible polyurethane coatings. Prog Org Coat 32 (1):65-71. https://doi.org/10.1016/S0300-9440(97)00076-3
23. Lomölder R, Plogmann F, Speier P (1997) Selectivity of isophorone diisocyanate in the urethane reaction influence of temperature, catalysis, and reaction partners. J Coat Technol Res 69 (868):51-57. https://doi.org/10.1007/BF02696250
24. Ono H-K, Jones FN, Pappas SP (1985) Relative reactivity of isocyanate groups of isophorone diisocyanate. Unexpected high reactivity of the secondary isocyanate group. Journal of Polymer Science: Polymer Letters Edition 23 (10):509-515. https://doi.org/10.1002/pol.1985.130231003
25. Hatada K, Ute K, Oka K-I et al (1990) Unambiguous 13C-NMR assignments for isocyanate carbons of isophorone diisocyanate and reactivity of isocyanate groups in Z - and E-stereoisomers. J Polym Sci, Part A: Polym Chem 28 (11):3019-3027. https://doi.org/10.1002/pola.1990.080281111
26. Wang L-M, Pan T-Y, Shi X-M et al (2005) Characterization of isophrone diisocyanate(IPDI) by NMR spectroscopy. Chinese Journal of Magnetic Resonance 22 (1):79-84. https://doi.org/10.3969/j.issn.1000-4556.2005.01.012
27. Zhang J, Yang K, Zhang Z et al (2019) Molecular structure characterization of hydroxyl-terminated hyperbranched polyester. Chinese Journal of Functional Polymers 32 (2):206-211,254. https://doi.org/10.14133/j.cnki.1008-9357.20180614002
28. Xing J, Ye Q (2003) Technical progress of the water dispersible polyisocyanates. Chemical Propellants and Polymeric Materials (in Chinese) 1 (4):15-18. https://doi.org/10.3969/j.issn.1672-2191.2003.04.006